AIR-TIGHT THREE-ELECTRODE DESIGN OF COAXIAL ELECTROCHEMICAL–EPR CELL FOR REDOX STUDIES AT LOW TEMPERATURES

František HARTL[1,*], Ronald P. GROENESTEIN[2] and Taasje MAHABIERSING[3]

Institute of Molecular Chemistry, University of Amsterdam, Nieuwe Achtergracht 166, NL-1018 WV Amsterdam, The Netherlands; e-mail: [1] hartl@anorg.chem.uva.nl, [2] groenest@chem.uva.nl, [3] taasje@anorg.chem.uva.nl

Received December 20, 2000
Accepted December 29, 2000

In memory of the late Professor Antonín A. Vlček, in recognition of his pioneering studies in the field of electrochemistry of coordination compounds.

The weak point of the original Allendoerfer electrochemical–EPR cell has been the reference electrode, placed outside the space-limited electrolysis cavity or not used at all in experiments at low temperatures. We present here an elegant solution to this problem, based on a modified air-tight design of an Allendoerfer cell equipped with a silver-wire pseudoreference electrode. The cell performance is demonstrated on one-electron electrochemical oxidation of heterocyclic 3,6-diphenyl-1,2-dithiine and one-electron reduction of 6-methyl-6-phenylfulvene and the pseudo-octahedral complex *fac*-[Re(benzyl)$(CO)_3$(dmb)] (dmb = 4,4′-dimethyl-2,2′-bipyridine). In the latter case, the EPR spectrum of the radical anion $[Re(benzyl)(CO)_3(dmb)]^{\bullet -}$ points to predominant localization of the unpaired electron on the dmb ligand, in agreement with UV-VIS and IR spectroelectrochemical data.

Keywords: Electron paramagnetic resonance; Electrochemistry; Low temperature; 1,2-Dithiine; Fulvene; Rhenium complex; Alkyl ligand.

The application of electron paramagnetic resonance (EPR) spectroscopy as a sensitive technique in electrochemical studies receives special attention each time when paramagnetic species with unpaired electron(s) (radicals) are produced in the course of electrode reactions. Careful analysis of the recorded EPR signal facilitates assignment of the radicals formed as stable compounds or reaction intermediates, and elucidation of their bonding properties[1]. In this regard it should be noted that also Prof. A. A.Vlček and co-workers devoted special attention to simultaneous electrochemical–EPR measurements[2a–2c]. In their redox studies of coordination and organometallic compounds, a flat EPR spectroelectrochemical cell was used, con-

doi: 10.1135/cccc20010052

structed by Klíma *et al.* in the late 1970's (refs[2d,2e]). As a matter of fact, it was the experience with the latter cell that stimulated our investigations in this area and has resulted in this contribution.

In situ electrolytic generation of radicals within the EPR cavity is convenient whenever their transfer after *external* (chemical, electrochemical) generation causes their rapid decomposition, *e.g.* due to extreme sensitivity to (adsorbed) oxygen or moisture, or requires complicated manipulations. This all applies, for example, to the metal-centred (d^7 Mn(0)) radical [Mn(3,5-di-*tert*-butylcatecholate)$(CO)_3$)]$^{2-}$ that could be electrogenerated within the aforementioned EPR spectroelectrochemical cell[3]. Frequently encountered thermal reactivity of radicals presents another need for application of *in situ* EPR techniques. Depending on their nature and lifetime, transient radicals can be detected with the aid of time-resolved (Fourier transform) EPR studies[4] or flow-through electrochemical–EPR techniques[5]. Stationary *in situ* electrolyses, producing unstable radicals, then demand construction of special EPR spectroelectrochemical cells that operate at sufficiently low temperatures[6].

Various designs of electrochemical–EPR cells have emerged since 1959 (ref.[7]). Regarding their drawbacks, they can be generally grouped into four categories:

a) *Flat thin-layer cells* cannot be used at low temperatures. They suffer from large ohmic resistance between the working and reference electrodes (*iR* drop) and from non-uniform current density (potential gradient) over the working electrode. Their response is usually slow.

b) *Flat, channel-flow cells*, moreover, require large sample volumes.

c) *Tubular, large-volume cells* cannot be used for solvents with large permittivity. They suffer from convective diffusion that sweeps radicals out of the EPR-active volume and/or annihilates them.

d) *Tubular, small-volume cells* (with a small working electrode) are rather fragile; they often possess low sensitivity, *i.e.* poor development of hyperfine splitting patterns, and EPR signal averaging at the applied constant electrode potential is required.

In 1975, Allendoerfer *et al.*[8] published a superior coaxial design of an electrochemical–EPR cell which attracted our attention. This cell has featured a gold-helical working electrode of a large active surface, fitted tightly against the inner wall of a 6-mm quartz tube. In this configuration, the microwaves penetrate only the thin solution layer between the gold helix and the inner wall, which permits virtually any material, *e.g.* a counter-electrode, to be placed inside the helix without affecting the EPR experiment. The *main advantages* of this design are (i) rapid electrolysis, (ii) uniform current

density, (iii) simple single-point potential control of the working electrode, (iv) high sensitivity, (v) undistorted EPR signal, (vi) utility even for highly polar solvents with large dielectric losses, such as acetonitrile, and (vii) easy dismantling and cleaning. However, the *principal drawback* of the original cell is the reference electrode (*e.g.* SCE), placed outside the space-limited electrolysis cavity and connected to the latter with a fragile Luggin capillary, thereby preventing EPR experiments to be undertaken over a wide temperature range. The cell hardly allows application of vacuum and can only be filled in a dry-box. It is therefore less suited for thermally unstable and highly oxygen- and moisture-sensitive radicals. Working at low temperatures with a two-electrode Allendoerfer-type cell[9] made the response of the large working electrode poor and seriously complicated multi-step eletrolysis, such as EPR studies of redox series.

In order to overcome the construction drawback of the original Allendoerfer cell, we had two principal tasks:

a) to place a suitable (single point) reference electrode inside the narrow electrolysis cavity at a fixed position and to insulate it from the counter-electrode metal;

b) to find the best position of the reference point relative to the gold-helix working electrode.

A solution to these problems, based on introduction of a pseudoreference silver-wire electrode, is presented hereinafter and the design of the modified Allendoerfer-type cell is described in detail. Illustrative examples of the cell performance at low temperatures have been taken from our recent electrochemical studies and will be introduced and discussed in separate sections.

EXPERIMENTAL

Materials and Preparations

Tetrahydrofuran (THF), dichloromethane (DCM) and butyronitrile (PrCN) (analytical grade, Acros) were dried using Na/benzophenone (THF) and CaH_2 (DCM, PrCN), and freshly distilled prior to the use under an atmosphere of dry nitrogen. Tetrabutylammonium hexafluorophosphate (TBAH; Aldrich) was recrystallized twice from absolute ethanol and dried prior to the use *in vacuo* at 80 °C for 10 h. Ferrocene (Fc; BDH) was used as received. The studied compounds 3,6-diphenyl-1,2-dithiine (ref.[10]) and 6-methyl-6-phenylfulvene (ref.[11]) were provided by Prof. H. Hennig, University of Leipzig and Dr M. Tacke, University College Dublin, respectively. The light-sensitive complex *fac*-[Re(Bn)$(CO)_3$(dmb)] (Bn = benzyl; dmb = 4,4′-dimethyl-2,2′-bipyridine) was prepared according to the literature procedure[12]; according to its IR spectrum and cyclovoltammetric response, the latter complex contained a small amount (<5%) of the precursor complex *fac*-[ReBr$(CO)_3$(dmb)].

Spectroscopy

IR spectra were recorded on a Bio-Rad FTS-7 spectrometer, UV-VIS spectra on a software-updated Perkin–Elmer Lambda 5 spectrophotometer, and X-band EPR spectra on a Varian Century E-104A spectrometer connected to a PC. EPR spectra were simulated with the PEST WinSim program[13], Version 0.96 (National Institute of Environmental Health Studies, New York).

Electrochemistry

The samples were prepared under an atmosphere of dry nitrogen, using standard Schlenk techniques.

Cyclic voltammetric measurements were performed with an EG&G PAR Model 283 potentiostat and an air-tight single-compartment three-electrode cell, equipped with a Pt disk (d = 0.8 mm) working, Pt-coil auxiliary and Ag-coil pseudoreference electrodes. Ferrocene (Fc) was used as internal standard[14]. Under the given experimental conditions, $E_{1/2}(Fc/Fc^+)$ = +0.575 V *vs* SCE in THF and +0.42 V *vs* SCE in DCM; ΔE_p = 90 mV. The working electrode surface was carefully polished between scans with a 0.5 μm diamond paste. The samples were typically *ca* 10^{-3} M in the studied compound and $3 \cdot 10^{-1}$ M in TBAH.

Spectroelectrochemical measurements were conducted with solutions containing $3 \cdot 10^{-1}$ M TBAH and $5 \cdot 10^{-3}$ M (IR) or $1 \cdot 10^{-3}$ M (UV-VIS, EPR) electrolyzed compound. Apart from the electrolyses with the electrochemical–EPR cell described hereinafter, the UV-VIS and IR spectroelectrochemical experiments were performed with the previously published optically transparent thin-layer electrochemical (OTTLE) cells[15]. Potential control during the electrolyses was achieved with a PA4 potentiostat (EKOM, Czech Republic).

RESULTS AND DISCUSSION

Description of the Modified Allendoerfer-Type Electrochemical–EPR Cell

In our construction, all the advantages of the original Allendoerfer electrochemical–EPR cell and its optimum performance (in particular rapid electrolysis on the whole working electrode surface and high sensitivity), as described elsewhere, have been preserved. In addition, and most importantly, access to low temperatures (down to 183 K in butyronitrile, the lowest temperature tested so far[1a]) has been obtained. The cell can be attached to a Schlenk line and does not require handling in a glove box. Details of the novel construction are depicted and described in Fig. 1.

The parameters of the working Au-helix electrode have remained unchanged: 48 turns per 3 cm total length, to give optimum EPR sensitivity. An auxiliary Pt-helix electrode has been employed instead of a Pt-foil cylinder; it is wound on a supporting glass rod at a fixed distance from the Au helix, thereby reducing the solution volume (see Fig. 1b).

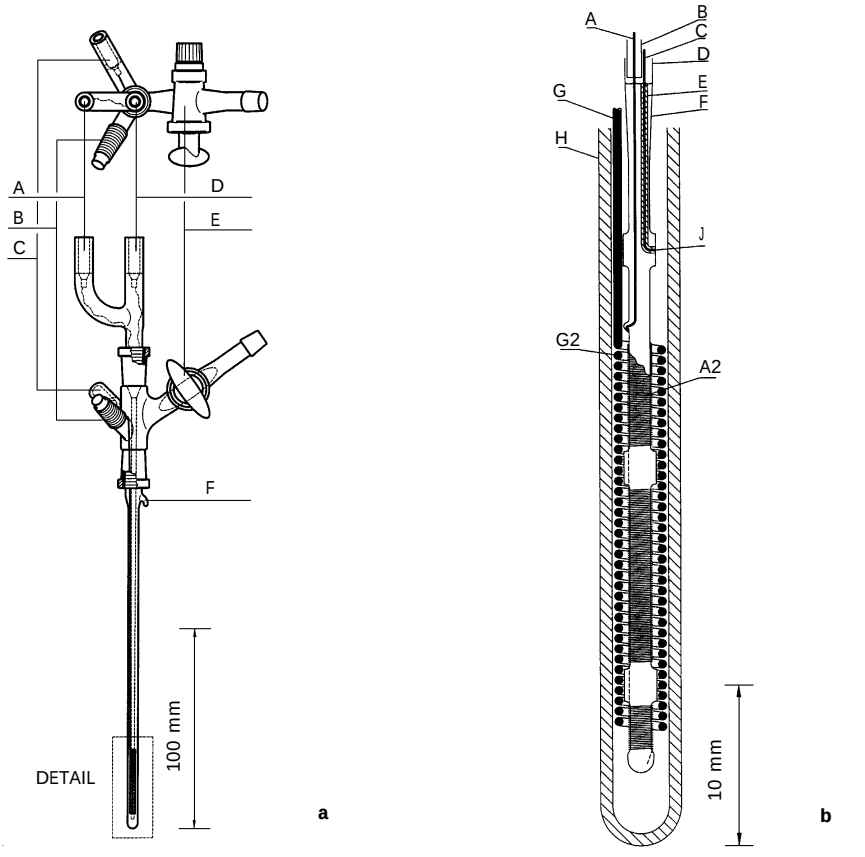

FIG. 1

Schematic representation of the novel three-electrode version of the Allendoerfer-type electrochemical–EPR cell. **a** Complete cell: A contact to Pt-helix counter-electrode; B filling port (*e.g.* through a rubber septum); C contact to the Au-helix working electrode; D contact to the Ag-wire pseudoreference electrode; E connection to a Schlenk line; F glass appendix serving for an elastic connection of the EPR tube with the glass arm of A. **b** Detail of the electrolysis cavity: A contact Pt wire (d = 0.1 mm) to the inner Pt-helix electrode; A_2 Pt-helix counter-electrode, wound on a supporting glass rod (Schott 8533 glass) with cut spacers (F); B glass tube insulating the Pt-counter-electrode wire from the Ag wire; C Ag wire (d = 0.1 mm) of the pseudoreference electrode; D inner glass tube carrying the contact wires of the counter- and pseudoreference electrode; E lead glass mantle insulating the Ag-wire pseudoreference electrode; it is melt-sealed into the Schott 8533 glass rod (F); F supporting glass rod; in the upper part with melt-sealed Pt and Ag contact wires, in the lower part with the wound Pt-helix counter-electrode; G contact wire (d = 0.5 mm) of the Au-helix working electrode; G_2 Au-helix working electrode (d = 3.2 mm, length of 3 cm, 16 turns per cm); H quartz EPR tube (outer diameter of 5 mm, inner diameter of 3.5 mm); J single-point Ag-wire pseudoreference electrode, protruding in the uppermost cut-glass spacer

Like in the other types of our spectroelectrochemical cells[15] (UV-VIS-NIR and IR), we have chosen for a tiny Ag-wire (d = 0.1 mm) pseudoreference electrode, allowing for fairly good potential control at given experimental conditions: the solvent used, temperature and concentration. As an insulating material, a special type of soft lead glass is used, permitting the Ag wire to be melt-sealed. The mantle of the lead glass can also readily be melt-sealed into a normal Pyrex glass, in this particular case Schott 8533, together with the Pt wire of the auxiliary electrode. In this way we have been able to manufacture a well-insulated single-point reference electrode perfectly suited for the coaxial electrode design (see part J in Fig. 1b).

In numerous tests, it turned out that the reference point needs to be placed slightly above the working electrode helix, in order to avoid a serious instability of the Ag pseudoreference electrode circuit under high-current conditions during electrolysis. Regardless of the increased distance, the potential control of the whole working electrode surface remained nearly unaffected.

In a typical experiment, the pre-dried cell parts were assembled, attached to a Schlenk line and repeatedly put under vacuum and an inert gas atmosphere. The cell tube can be filled simply with a syringe through a rubber septum. The solution level should rise slightly above the single Ag reference point. Small gas bubbles sometimes remaining at the Au electrode surface can easily be removed by repeated vertical motion of the central unit A/D in Fig. 1a under inert-gas stream protection. The cell is completely leak-proof and, while under an overpressure of an inert gas (not necessarily argon), it can be transferred to the EPR spectrometer cavity without any special precautions. A flow-through Dewar-type holder, made of quartz, was placed in the resonator for experiments at low temperatures. The cell is then chilled to a pre-selected temperature by passing a cold nitrogen stream along the tubular electrode compartment. The inner Dewar tube diameter slightly exceeds that of the cell tube, allowing facile tuning of the cavity properties to achieve resonance even for highly polar solvents with relatively large dielectric losses and, at the same time, to stick on an external g-standard label (2,2′-diphenyl-1-picrylhydrazyl, DPPH). When positioned properly in the resonance cavity, the cell was connected to a potentiostat. The electrolysis experiment started at a rest potential and well-defined cyclic voltammogram was recorded to localize the studied Faradaic process, usually with a scan rate of 5 mV s^{-1}; although, the scan rate (dependent on the iR drop) was not the limiting factor of the coaxial cell performance. Electrolyses with the cell proceeded rapidly (within *ca* 30 s limit), in particular for chemically reversible processes and well conducting solvents. They

start on the whole working electrode surface, as could indeed be checked visually by changed colour of the thin solution layer. Measurements at low temperatures are convenient even for completely chemically reversible redox pairs, as the convective diffusion, recognized as a serious problem in the original Allendoerfer cell, is much lower and the loss in EPR signal due to the solution circulation is fairly negligible. For one-electron Nernstian redox process, the electrolysis time delay at low temperatures is not significant compared with the electrolysis at 293 K, and the cyclic voltammograms remain nearly unaffected. After the experiment, the cell is easy to dismantle and clean.

Examples of the Electrochemical–EPR Cell Performance

Three different compounds have been studied with the newly developed electrochemical–EPR cell, aimed at demonstration of its merits and reliable performance. The results of the *in situ* electrolyses are presented in the following sections.

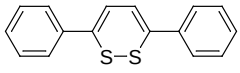

3,6-diphenyl-1,2-dithiine

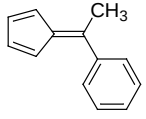

6-methyl-6-phenylfulvene

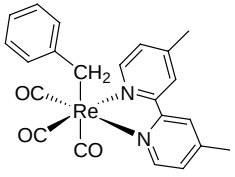

fac-[Re(Bn)(CO)$_3$(dmb)]

Thermally Unstable Radical Cation of 3,6-Diphenyl-1,2-dithiine

In the presence of oxidants, heterocyclic 1,2-dithiines photochemically form dithiapyrylium cations[16]. Electrochemical studies, including oxidative EPR spectroelectrochemistry, have been performed to elucidate the photoreaction pathways[17]. These studies have shown that one-electron oxidation of 3,6-diphenyl-1,2-dithiine in dichloromethane to the corresponding radical cation at $E_{1/2}$ = +0.665 V *vs* Fc/Fc$^+$, is reversible at 293 K on the time scale of cyclic voltammetry defined by scan rate ≥100 mV s^{-1}. However, thermal decomposition of the radical cation occurs at ambient temperature on a longer time scale of minutes, reflected in the disappearance of its nπ^* visible absorption band at 515 nm. UV-VIS spectroelectrochemistry confirmed inherent stability of the radical cation in dichloromethane at 233 K.

The same experimental conditions were therefore chosen also for the ESR studies, demanding application of the LT EPR spectroelectrochemical cell.

The well-developed EPR spectrum of the radical cation of 3,6-diphenyl-1,2-dithiine in dichloromethane at 233 K is depicted in Fig. 2. The excellent cell performance has been illustrated by rapid appearance of the EPR signal at the potential of the anodic wave of the parent compound, high signal intensity and large signal-to-noise ratio, and stability over a period of *ca* 30 min, reflecting limited convective-diffusion loss at low temperatures. As expected, the two equivalent hydrogen nuclei on the disubstituted 1,2-dithiine ring cause hyperfine splitting of the EPR signal giving the 1 : 2 : 1 triplet pattern, with a(H) = 0.35 mT. The additional splitting due to the ^{1}H nuclei of the phenyl substituents is limited and remains unresolved, pointing to a predominant localization of the unpaired electron on the sulfur atoms. MO calculations are in progress[17] to clarify whether the determined value of the a(H) constant is compatible with the expected planar structure of the one-electron-oxidized 1,2-dithiine ring, arising from the delocalized π-bonding.

Thermally Unstable Radical Anion of 6-Methyl-6-phenylfulvene

The redox behaviour of a series of substituted fulvenes and benzofulvenes has been investigated for their reductive dimerization producing *ansa*-metallocenes[18]. Their reactivity, induced upon one-electron reduction to the corresponding radical anions, plays a key role for the selectivity of these

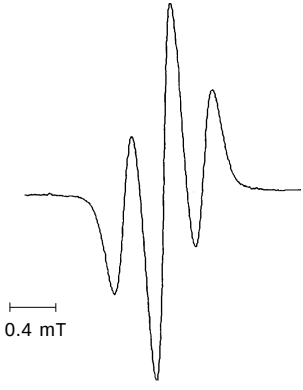

FIG. 2
EPR spectrum of the radical cation [3,6-diphenyl-1,2-dithiine]$^{\bullet+}$ electrogenerated *in situ* in dichloromethane at 233 K

syntheses. Here we present details for 6-methyl-6-phenylfulvene (MePhFv) and its radical anion, investigated with cyclic voltammetry, UV-VIS spectroelectrochemistry and EPR spectroscopy.

According to the cyclic voltammetric response, MePhFv is reduced reversibly at $E_{1/2}$ = –2.15 V *vs* Fc/Fc^+ at $\nu \geq 50$ mV s^{-1} (in THF at ambient temperature). The corresponding UV-VIS spectroelectrochemical experiments proved that the radical anion $[MePhFv]^{\bullet-}$, identified according to the characteristic sharp absorption band at 435 nm (Fig. 3), decomposes at 293 K within a few minutes but becomes inherently stable at 243 K (see inset to Fig. 3). In butyronitrile, the decomposition is much faster and $[MePhFv]^{\bullet-}$ could only be observed as a transient species even at 193 K. Further characterization of the radical anion with EPR spectroscopy was therefore attempted in THF at 223 K, using the novel electrochemical–EPR cell. The resulting well-resolved EPR signal is shown in Fig. 4. Its simulation has been a rather difficult task, as the signal possesses an irregular shape and several combinations of hydrogen hyperfine splitting constants give fairly similar results. The closest resemblance between the experimental and simulated spectra has been achieved with the following *a*(H) values (in mT): 0.971 (2×), 0.967, 0.426, 0.412, 0.340, 0.332, 0.312, 0.132, 0.124, 0.105 and

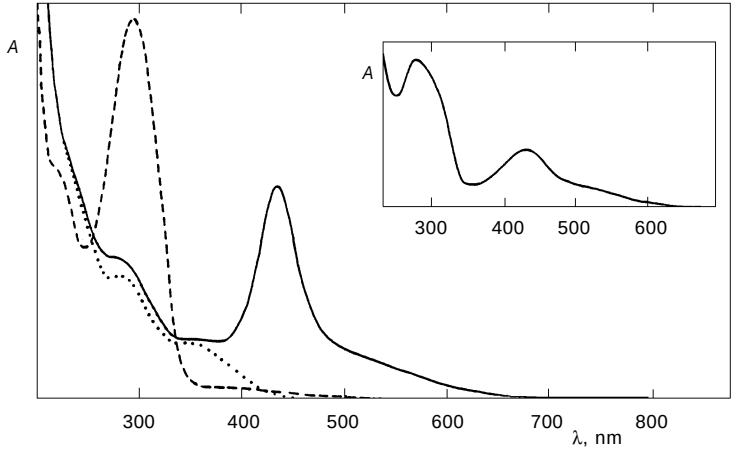

FIG. 3
UV-VIS spectra of 6-methyl-6-phenylfulvene, MePhFv (– – –), $[MePhFv]^{\bullet-}$ (———) electrogenerated in an OTTLE cell[15a], and a thermal decomposition product (· · · ·) in THF at 293 K. Inset: UV-VIS spectrum of stable $[MePhFv]^{\bullet-}$ electrogenerated in an OTTLE cell[15b] in THF at 243 K

0.092. Apparently, support from theoretical MO calculations is needed to facilitate assignment of these EPR data and to discuss their relevance to the electronic structure of $[MePhFv]^{\bullet -}$.

Bonding Properties of the Radical Anion fac-[Re(Bn)(CO)$_3$(dmb)]$^{\bullet -}$

Complexes *fac*-[Re(R)(CO)$_3$(α-diimine)] (R = covalently bound alkyl group) have been the subject of detailed spectroscopic studies in our laboratory due to their intriguing photochemistry[12,19]. The results have been periodically reviewed[20]. In general, photoexcitation into the lowest metal-to-ligand charge transfer band, followed by population of a dissociative $^3\sigma$(Re–R)π*(α-diimine) (SBLCT) excited state, results in homolysis of the Re–alkyl bond and efficient formation of radicals. In this regard it is interesting to investigate whether similar reactivity is induced electrochemically, upon one-electron reduction producing the radical anions $[Re(R)(CO)_3(\alpha\text{-diimine})]^{\bullet -}$.

The first spectroelectrochemical experiments (UV-VIS, IR, EPR) were performed by Rossenaar *et al.* with a series of complexes *fac*-[Re(R)(CO)$_3$(iPr-DAB)] (R = Me, Et, Bn; iPr-DAB = 1,4-diisopropyl-1,4-diazabutadiene)[21]. These complexes could be reduced in the available potential window in a *single* cathodic step to give surprisingly stable radical anions, formulated tentatively as $\{[Re(CO)_3(\alpha\text{-diimine})]^{-}...R^{\bullet}\}$. These compounds resemble electronically the two-electron-reduced five-coordinate anions $[Re(CO)_3(iPr\text{-}DAB)]^{-}$, with the $R^{\bullet}$ radical group in the vicinity of the Re centre. Support for this

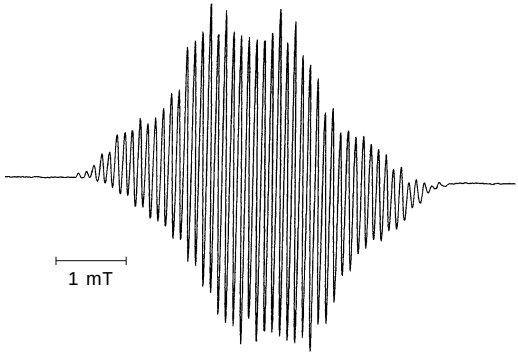

FIG. 4
EPR spectrum of the radical anion $[MePhFv]^{\bullet -}$ electrogenerated *in situ* in THF at 223 K

assignment has come from the spectroelectrochemical data (in THF). For example, the radical anion {$[Re(CO)_3$(iPr-DAB)$]^-$...$Me^\bullet$} absorbs in the visible spectral region at 400 nm and its IR CO-stretching bands are found at 1 955 (s) and 1 828 (vs, br) cm^{-1}. For the anion $[Re(CO)_3$(iPr-DAB)$]^-$ the corresponding values are very similar: 440 nm, and 1 942 (s) and 1 825 (vs, br) cm^{-1}. Conclusive evidence for the radical anionic nature of {$[Re(CO)_3$(iPr-DAB)$]^-$...$R^\bullet$} has been obtained from EPR spectroscopy. The EPR signal of {$[Re(CO)_3$(iPr-DAB)$]^-$...$Et^\bullet$} is a sextet with a relatively large ^{185,187}Re hyperfine splitting (a(Re) = 4.87 mT), and obscured hyperfine splitting due to the ethyl group[21].

In order to clarify the bonding situation in the alkyl-rhenium α-diimine radical-anionic complexes, the comparative spectroelectrochemical studies have been extended to the complex *fac*-[Re(Bn)$(CO)_3$(dmb)] (IR ν(CO) bands at 1 992.5 and 1 881.5 (br) cm^{-1} (in THF)). The cyclic voltammogram of the latter complex shows fully reversible one-electron reduction at $E_{1/2}$ = –2.08 V *vs* Fc/Fc^+, followed by an irreversible cathodic step at $E_{p,c}$ = –2.84 V (in THF, 293 K). IR spectroelectrochemistry has revealed that the *first* cathodic step produces a species with ν(CO) bands shifted to 1 971 and 1 854/1 840 (sh) cm^{-1}; for the *second* cathodic step further shift of the ν(CO) bands down to 1 944 and 1 842 cm^{-1} was observed. Comparison of the IR ν(CO) data with the UV-VIS spectra of these two reduction products (Fig. 5) then allows their unambiguous assignment to the one-electron-reduced radical anion $[Re(Bn)(CO)_3(dmb)]^{\bullet-}$ and the two-electron-reduced five-coordinate anion $[Re(CO)_3(dmb)]^-$, respectively. In particular, the UV-VIS spectrum of $[Re(Bn)(CO)_3(dmb)]^{\bullet-}$ exhibits characteristic[22] structured absorption bands due to π*π* intraligand electronic transitions of the radical anionic $[dmb]^{\bullet-}$ ligand at 511 and 543 nm (allowed) and below 650 nm (forbidden) (Fig. 5a). In the UV-VIS spectrum of the anion $[Re(CO)_3(dmb)]^-$ the intense structured band at 545 nm corresponds to several electronic transitions within the strongly π-delocalized (carbonyl)Re–dmb system[23] (Fig. 5b).

These results point to a remarkable difference between the non-aromatic iPr-DAB and aromatic dmb ligands in the radical-anionic complexes. The dmb ligand is apparently better suited to accommodate the unpaired electron in its π*-system, leaving the Re–alkyl bond in the radical-anionic complex intact. Dissociation of the alkyl ligand is only induced by the second one-electron cathodic step. This is in sharp contrast with the initial one-electron reduction of [Re(R)$(CO)_3$(iPr-DAB)] containing the non-aromatic iPr-DAB ligand, that results in significant weakening of the Re–alkyl bond.

The EPR spectrum of the radical anion $[Re(Bn)(CO)_3(dmb)]^{\bullet -}$, recorded with the light-protected electrochemical–EPR cell in the course of the one-electron reduction of the parent complex in THF at 223 K (giving higher signal intensity), shows a poorly resolved sextet due to $^{185,187}Re$ hyperfine splitting (Fig. 6). Simulation of the spectrum provided the value a(Re) = 2.10 mT, which is significantly smaller than the rhenium hyperfine

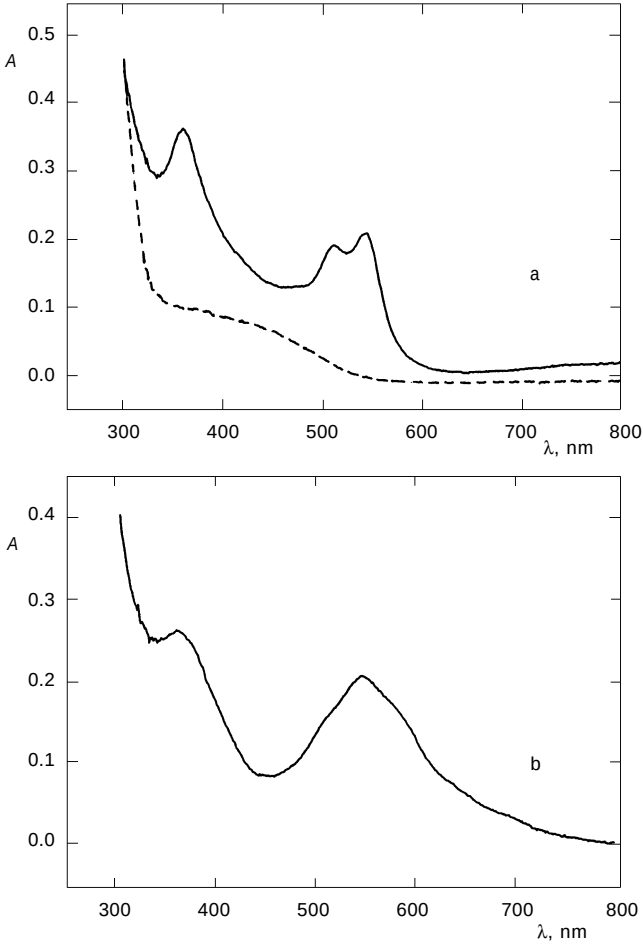

FIG. 5

UV-VIS spectra of: a $[Re(Bn)(CO)_3(dmb)]$ (– – –) and its radical anion (——) in THF at 293 K; b the five-coordinate anion $[Re(CO)_3(dmb)]^-$ in THF at 293 K. The one- and two-electron-reduced complexes were electrogenerated in an OTTLE cell[15a]

splitting observed for {[$Re(CO)_3$(iPr-DAB)]$^-$...Et$^\bullet$}. This result is therefore in agreement with the predominant localization of the unpaired electron on the dmb ligand and stronger Re–alkyl bond in the singly reduced dmb complexes. Similar, even though less pronounced difference in the bonding properties is also found for corresponding radical-anionic rhenium-halide complexes[22b,24].

In conclusion, the presented EPR spectra of the three different radicals demonstrate that the newly developed air-tight three-electrode Allendoerfer-type (coaxial) electrochemical–EPR cell enables high quality EPR spectra to be recorded at low temperatures. The signal-to-noise ratio can further be improved by signal averaging. The specially designed single-point Ag pseudoreference electrode in the proximity of the working Au-helix electrode allows an effective potential control under given experimental conditions. This major improvement of the original design of the Allendoerfer cell extends its applicability[8] also to the field of variable-temperature studies.

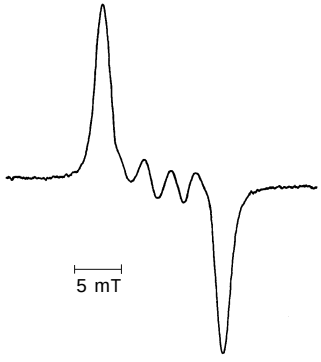

FIG. 6
EPR spectrum of the radical anion [$Re(Bn)(CO)_3$(dmb)]$^{\bullet-}$ electrogenerated *in situ* in THF at 223 K

Prof. H. Hennig (University of Leipzig), Dr M. Tacke (University College Dublin) and Dr C. J. Kleverlaan (University of Amsterdam) are acknowledged for the generous gift of the compounds selected as characteristic examples of the cell performance. We are also grateful to Mr H. Luyten and Mr G. Braspenning (both University of Amsterdam) for their assistance and stimulating discussions during the cell development.

REFERENCES

1. a) Farell I. R., Hartl F., Záliš S., Mahabiersing T., Vlček A., Jr.: *J. Chem. Soc., Dalton Trans.* **2000**, 4323; b) Aarnts M. P., Wilms M. P., Peelen K., Fraanje J., Goubitz K., Hartl F., Stufkens D. J., Baerends E. J., Vlček A., Jr.: *Inorg. Chem.* **1996**, *35*, 5468; c) Mevs J. M., Geiger W. E.: *Organometallics* **1996**, *15*, 2350; d) Webster R. D.: *J. Chem. Soc., Perkin Trans. 2* **1999**, 263.
2. a) Miholová D., Klíma J., Vlček A. A.: *Inorg. Chim. Acta* **1978**, *27*, L67; b) Gaš B., Klíma J., Záliš S., Vlček A. A.: *J. Electroanal. Chem.* **1987**, *222*, 161; c) Miholová D., Gaš B., Záliš S., Klíma J., Vlček A. A.: *J. Organomet. Chem.* **1987**, *330*, 75; d) Ludvík J., Klíma J., Volke J., Kurfürst A., Kuthan J.: *J. Electroanal. Chem.* **1982**, *138*, 131; e) Klíma J., Volke J., Urban J.: *Electrochim. Acta* **1991**, *36*, 73.
3. Hartl F., Vlček A., Jr.: *Inorg. Chem.* **1991**, *30*, 3048.
4. a) van Slageren J., Martino D., Kleverlaan C. J., Bussandri A. P., van Willigen H., Stufkens D. J.: *J. Phys. Chem. A* **2000**, *104*, 291; b) Sakaguchi Y., Hayashi H., I'Haya Y. J.: *J. Phys. Chem.* **1990**, *94*, 291.
5. Bagchi R. N., Bond A. M., Scholz F.: *J. Electroanal. Chem.* **1988**, *252*, 259.
6. a) Mu X. H., Kadish K. M.: *Electroanalysis* **1990**, *2*, 15; b) Macgregor S. A., McInnes E., Sorbie R. J., Yellowlees L. J. in: *Molecular Electrochemistry of Inorganic, Bioinorganic and Organometallic Compounds* (A. J. L. Pombeiro and J. A. McCleverty, Eds), p. 503. Kluwer Academic Publishers, Dordrecht 1993; c) Kaim W., Ernst S., Kasack V.: *J. Am. Chem. Soc.* **1990**, *112*, 173.
7. Webster R. D., Bond A. M., Coles B. A., Compton R. G.: *J. Electroanal. Chem.* **1996**, *404*, 303; and refs[4–11] therein.
8. Allendoerfer R. D., Martinchek G. A., Bruckenstein S.: *Anal. Chem.* **1975**, *47*, 890.
9. Hartl F.: *Inorg. Chim. Acta* **1995**, *232*, 99.
10. Schroth W., Hintzsche E., Spitzner R., Stroehl D., Sieler J.: *Tetrahedron* **1995**, *51*, 13247.
11. Stone K. J., Little R. D.: *J. Org. Chem.* **1984**, *49*, 1849.
12. Kleverlaan C. J., Stufkens D. J.: *Inorg. Chim. Acta* **1999**, *284*, 61.
13. Duling. D. R.: *J. Magn. Reson., Ser. B* **1994**, *104*, 105.
14. Gritzner G., Kůta J.: *Pure Appl. Chem.* **1984**, *56*, 461.
15. a) Krejčík M., Daněk M., Hartl F.: *J. Electroanal. Chem.* **1991**, *317*, 179; b) Hartl F., Luyten H., Nieuwenhuis H. A., Schoemaker G. C.: *Appl. Spectrosc.* **1994**, *48*, 1522.
16. Schumer F., Hennig H.: Personal communication.
17. Hennig H., Schroth W., Schumer F., Kaden H., Gelssner W., Mahabiersing T., Hartl F.: Unpublished results.
18. Tacke M., Fox. S., Cuffe L., Dunne J. P., Hartl F., Mahabiersing T.: *J. Mol. Struct.* **2001**, *559*, 331.
19. a) Lucia L. A., Burton R. D., Schanze K. S.: *Inorg. Chim. Acta* **1993**, *208*, 103; b) Rossenaar B. D., Kleverlaan C. J., van de Ven M. C. E., Stufkens D. J., Vlček A., Jr.: *Chem.-Eur. J.* **1996**, *2*, 228; c) Farrel I. R., Matoušek P., Kleverlaan C. J., Vlček A., Jr.: *Chem.-Eur. J.* **2000**, *6*, 1386.
20. Stufkens D. J., Aarnts M. P., Nijhoff J., Rossenaar B. D., Vlček A., Jr.: *Coord. Chem. Rev.* **1998**, *171*, 93.
21. Rossenaar B. D., Hartl F., Stufkens D. J.: *Inorg. Chem.* **1996**, *35*, 6194.
22. a) Víchová J., Hartl F., Vlček A., Jr.: *J. Am. Chem. Soc.* **1992**, *114*, 10903; b) Rossenaar B. D., Stufkens D. J., Vlček A., Jr.: *Inorg. Chim. Acta* **1996**, *247*, 247.

23. a) Stor G. J., Hartl F., van Outersterp J. W. M., Stufkens D. J.: *Organometallics* **1995**, *14*, 1115; b) Rossenaar B. D., Hartl F., Stufkens D. J., Amatore C., Maisonhaute E., Verpeaux J.-N.: *Organometallics* **1997**, *16*, 4675; c) Hartl F., Le Floch P., Rosa P., Záliš S.: Unpublished results.
24. Klein A., Vogler C., Kaim W.: *Organometallics* **1996**, *15*, 236.